

Preparation and modification of high performance porous carbons from petroleum coke for use as supercapacitor electrodes

Ming-hui Tan^{1,2}, Peng Li¹, Jing-tang Zheng¹, Tsubaki Noritatsu^{2*}, Ming-bo Wu^{1*}

¹State Key Laboratory of Heavy Oil Processing, China University of Petroleum, Qingdao 266580, China;

²Department of Applied Chemistry, Graduate School of Engineering, University of Toyama, Gofuku 3190, Toyama 930-8555, Japan

Abstract: As a byproduct of oil refining, petroleum coke with a high carbon content (about 90 wt%) has been shown to be a good raw material for porous carbons (PCs). PCs with high specific surface areas were derived from petroleum coke by KOH activation. The effect of KOH/coke mass ratio on the pore structure of the PCs and their electrochemical performance as electrodes of electric double layer capacitors were investigated. Results showed that the specific surface area and pore size distribution of the PCs could be efficiently controlled by the KOH/coke ratio. The pore sizes of the PCs increase with increasing KOH/coke ratio, and the largest specific surface area was as high as 2964 m²·g⁻¹. A PC-5 electrode prepared with a KOH/coke ratio of 5:1 has a high specific surface area of 2842 m²·g⁻¹ and mesoporosity of 67.0 %, and has the largest specific capacitance at all investigated current densities among the PCs examined. This is ascribed to its high specific surface area and high mesoporosity. Hydrothermal modification of PC-3 (KOH/coke ratio at 3:1) in ammonia at 200 °C increases its specific capacitance, especially at high discharge current densities. This improved electrochemical performance can be attributed to nitrogen-doping that occurs during the process, and this can induce pseudo-capacitance and improve the hydrophilicity of the PC electrode to the electrolyte. KOH activation combined with ammonia hydrothermal modification is a simple yet efficient approach to prepare cost-effective PCs for supercapacitors with excellent electrochemical performance.

Key Words: Petroleum coke; Porous carbon; Supercapacitors; Ammonia hydrothermal modification; Nitrogen doping

1 Introduction

Electric double-layer capacitors (EDLCs) have attracted much attention as attractive energy storage devices owing to their high power density and excellent cycling stability^[1-3]. EDLCs store energy mainly via forming electric double layers (EDLs) on the electrode/electrolyte interface, thus their electrochemical performance highly depend on the available surface area of electrode materials^[4-6]. Porous carbons (PCs) have been widely used as electrode materials for commercial EDLCs owing to their relatively large specific surface area, good chemical stability, and a wide range of application temperatures^[7-10].

Generally, the larger the specific surface area of the PC is, the higher specific capacitance will be obtained according to the equation below^[11]:

$$C = \epsilon A / d \quad (1)$$

Where, A is the available surface area to electrolyte ions, ϵ is the electrolyte dielectric constant, and d is the separation between electrolyte ions and carbon surface. The values of A and d depend on the specific surface area and pore size of

electrode materials. PCs with high specific surface areas usually have relatively low capacitance than expected, due to a lot of ultramicropores (smaller than 0.7 nm) inaccessible to form EDLCs. Although the pores larger than the size of the electrolyte ions and their solvation shell are required for high value of A , the larger pores will certainly decrease the total specific surface area of PCs and increase the value of d , leading to an impressive power density but a low energy density. Therefore, an appropriate pore size distribution is very important for electrode materials to have excellent electrochemical performance. Many studies focus on template methods to produce controllable pores in the range of 2 to 4 nm^[12-14]. However, the complicated preparation procedure, high cost and low yield of PCs make the template methods difficult to achieve practical applications^[15-17]. Moreover, the micropores larger than 0.7 nm are proved available for electro-adsorption of hydrated ions in aqueous electrolytes^[11, 18]. Therefore, PCs having lots of mesopores and a certain amount of micropores prepared from inexpensive raw material via simple methods may have excellent electrochemical performance and promising applications in EDLCs. Besides

Received date: 10 May 2016; Revised date: 10 June 2016

*Corresponding author. E-mail: wumb@upc.edu.cn; tsubaki@eng.u-toyama.ac.jp

Copyright©2016, Institute of Coal Chemistry, Chinese Academy of Sciences. Published by Elsevier Limited. All rights reserved.

DOI: 10.1016/S1872-5805(16)60018-5

the pore structure, the surface properties also play important roles in improving the electrochemical performance of PCs. As an effective method, nitrogen-doping has received much attention and is often used to enhance the specific capacitance of electrode based on PCs^[19-22].

In this paper, petroleum coke was used as raw material to prepare PCs for EDLCs by KOH activation. Ammonia hydrothermal treatment on PCs was further used to improve the EDLC electrochemical performance. As a byproduct of oil refinery, petroleum coke has a high carbon content (about 90 wt%) and has been proved suitable raw material for PC preparation^[23, 24]. The relationships among the KOH/coke ratio, the pore structure and the electrochemical performance were discussed. Ammonia hydrothermal treatment is an efficient approach to dope nitrogen on PCs and enhance the electrochemical performance of PC electrodes.

2 Experimental

Petroleum coke from Daqing Oilfield of China was used as raw material to prepare PCs. The proximate and elemental analysis are listed in Table 1^[25].

PCs were prepared from petroleum coke with particle diameter smaller than 100 μm by KOH activation, using a mass ratio of KOH to petroleum coke of 1 to 5. The carbonization and activation were carried out in a horizontal tube furnace, where the samples were heated from room temperature to 500 $^{\circ}\text{C}$ at 5 $^{\circ}\text{C}\cdot\text{min}^{-1}$ and kept for 1 h, then heated to 850 $^{\circ}\text{C}$ at 5 $^{\circ}\text{C}\cdot\text{min}^{-1}$, and kept for 1.5 h. The above processes were performed under nitrogen flow of 60 $\text{mL}\cdot\text{min}^{-1}$ to protect the samples from oxidation. According to the mass ratio of KOH to petroleum coke ($m_{\text{KOH}}/m_{\text{petroleum coke}}$), the obtained samples were denoted as PC-1, PC-2, PC-3, PC-4 and PC-5.

In order to further increase the electrochemical performance of the PC electrodes, the PCs were hydrothermally treated in ammonia at different temperatures. PC-3 was mixed with ammonia, then placed into a hydrothermal reactor, and kept for 24 h at different temperatures. After the hydrothermal treatment, the samples were rinsed with distilled water, and then dried in an oven at 110 $^{\circ}\text{C}$. According to the temperature of hydrothermal treatment, hydrothermal treated PC-3 samples were named as PC-3-RT (room temperature), PC-3-100 (100 $^{\circ}\text{C}$), PC-3-150 (150 $^{\circ}\text{C}$) and PC-3-200 (200 $^{\circ}\text{C}$).

N_2 adsorption-desorption was carried out on a Micromeritics ASAP 2020 sorption analyzer (USA) to determine the BET specific surface areas and the pore size distributions of PCs. The crystal structures of samples were confirmed by X-Ray diffraction (XRD) (Rigaku RINT 2400, Japan). The surface morphology was characterized by scanning electron microscopy (SEM) (JEOL JSM-6360LV SEM, Japan) and transmission electron microscopy (TEM) (JEM-2100UHR, Japan). The temperature programmed desorption of carbon dioxide (CO_2 -TPD) was conducted by a Catalyst Analyzer BELCAT-B (Japan) with a heating rate of 10 $^{\circ}\text{C}\cdot\text{min}^{-1}$ to measure the intensity of basic sites of samples. X-ray photoelectron spectra (XPS) were recorded on a ESCALAB 250Xi spectrometer (Thermo Scientific, USA).

The electrodes were prepared from PCs by adding polytetrafluoroethylene emulsion (PTFE) as binder and acetylene black as conductive agent with a PC/acetylene black/PTFE mass ratio of 85/5/10. The mixture was pressed on the foam nickel with diameter of 12 mm at 20 MPa for 30 s, and then dried at 100 $^{\circ}\text{C}$ for 1 h in vacuum. Finally, button-type capacitor was assembled with two PC electrodes separated by a polypropylene membrane, using a 6 M KOH aqueous solution as an electrolyte. Galvanostatic charge/discharge analysis was carried out on a land cell tester (Land, CT-2001A, China). The cyclic voltammetry (CV) and electrochemical impedance spectroscopy (EIS) were performed on an electrochemical workstation (PARSTAT 4000, Princeton, USA). The potential range of CV was 0-1 V, and the Nyquist plot was recorded at the frequency from 100 kHz to 0.01 Hz. All electrochemical measurements were carried out at room temperature.

3 Results and discussion

The N_2 adsorption-desorption isotherms obtained at 77 K for PCs with different KOH/coke ratios are shown in Fig. 1a. PC-1 and PC-2 exhibit a typical type-I isotherm with a sharp increase in the amount of nitrogen adsorbed at low relative pressure until a plateau is formed and no obvious hysteresis loop is observed at high relative pressure. It is well known that the adsorption of microporous material at low p/p_0 is micropore filling. For PC-1 and PC-2, the plateaus are formed immediately following the quick increase. Compared to PC-1 and PC-2, the plateaus of PC-3, PC-4 and PC-5 are formed

Table 1 The basic properties of petroleum coke.

| Raw material | Proximate analysis, (wt%) | | | Elemental analysis, (wt%) | | | | |
|----------------|---------------------------|------------------|-----------------|---------------------------|------|------|------|------|
| | A_d | V_{daf} | M_{ad} | C | H | S | N | O |
| Petroleum coke | 0.21 | 12.49 | 1.20 | 90.30 | 4.26 | 0.81 | 1.79 | 2.84 |

* A_d : the ash content in petroleum coke on the dry basis; M_{ad} : the water content in petroleum coke on the air dry basis;

V_{daf} : the volatile matter content in petroleum coke on dry and ash free basis

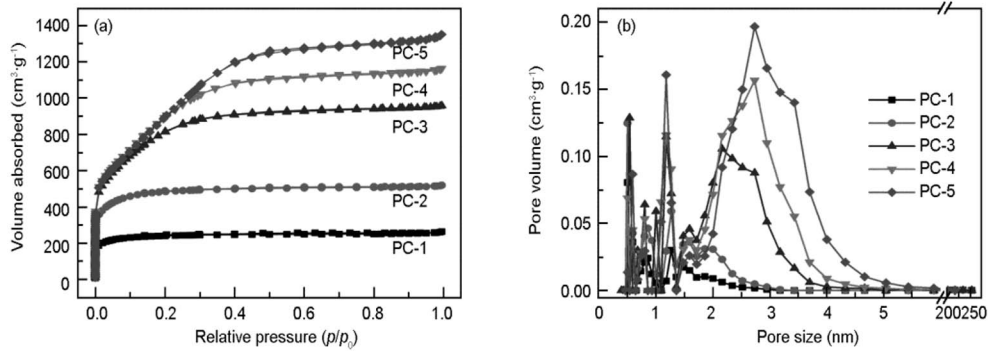


Fig. 1 (a) N_2 adsorption-desorption isotherms and (b) pore size distributions of PCs.

Table 2 Pore parameters and yields of PCs.

| PCs | S_{BET} , ($\text{m}^2 \cdot \text{g}^{-1}$) | Pore volume, $\text{cm}^3 \cdot \text{g}^{-1}$ | | | $V_{\text{mic}}/V_{\text{t}}$, (%) | $V_{\text{mes}}/V_{\text{t}}$, (%) | D_{ap} , (nm) | Yield, (%) |
|------|--|--|------------------|------------------|--|--|---------------------------|---------------|
| | | V_{t} | V_{mic} | V_{mes} | | | | |
| PC-1 | 906 | 0.34 | 0.31 | 0.03 | 91.2 | 8.8 | 1.72 | 77.1 |
| PC-2 | 1841 | 0.68 | 0.61 | 0.07 | 89.7 | 10.3 | 1.76 | 64.5 |
| PC-3 | 2964 | 1.25 | 0.76 | 0.49 | 60.8 | 39.2 | 1.99 | 59.8 |
| PC-4 | 2914 | 1.53 | 0.70 | 0.83 | 45.8 | 54.2 | 2.45 | 44.4 |
| PC-5 | 2842 | 1.76 | 0.58 | 1.18 | 33.0 | 67.0 | 2.90 | 35.2 |

* S_{BET} : the BET specific surface area; V_{t} : the total pore volume; V_{mic} : the micropore volume; V_{mes} : the mesopore volume (Due to the very low content, the macropore volume was included in mesopore.); D_{ap} : the average pore diameter; Yield: the percentage of PC obtained per initial weight of petroleum coke.

more slowly and the knees of the isotherms become wider successively as KOH/coke ratio increases from 3:1 to 5:1. In the case of PC-5, the plateau forms till 0.4 of the relative pressure. The saturation steps become long and the slopes of the plateaus increase due to multi-layer adsorptions of wide micropores and narrow mesopores^[26], revealing that the pore size distribution of PCs becomes wide when more KOH is used.

The pore size distributions of PCs calculated from the adsorption branch by Density Functional Theory method are given in Fig. 1b, which clearly reveals the change on the pore size at different KOH/coke ratios. It can be seen that all PCs have similar pore size distributions in microporous range (less than 2 nm). Meanwhile, PCs at higher KOH/coke ratios (e.g. 3:1, 4:1 and 5:1) have much more mesopores and larger volume in mesopore range (2-50 nm). The pore size becomes wide gradually with increasing KOH/coke ratio, indicating the pore size distributions of PCs could be finely controlled by the mass ratio of KOH/petroleum coke.

It is obviously seen that the adsorption amounts of N_2 increase greatly as the KOH/coke ratio increases from 1:1 to 5:1 in Fig. 1a, revealing that the BET surface area and pore volume of PCs increase remarkably (Table 2) with the KOH/coke ratio. The specific surface area increases from 906 to 1841 $\text{m}^2 \cdot \text{g}^{-1}$ as KOH/coke ratio increases from 1:1 to 2:1, while the pore volume increases from 0.40 to 0.61 $\text{cm}^3 \cdot \text{g}^{-1}$. Taken into consideration that PC-1 and PC-2 belong to microporous materials, it is clearly proved that more KOH

used can generate more micropores, and the surface area and pore volume increase accordingly. As KOH/coke ratio increases from 2:1 to 3:1, the specific surface area and pore volume keep increasing. The pore volume especially mesopore volume increases much more sharply, indicating that the abundant KOH at high KOH/coke ratio not only generates more new micropores, but also enlarges the primary pores to form mesopores. When the KOH/coke ratio increases from 3:1 to 5:1, the specific surface area and the micropore volume slightly decrease and the total pore volume keeps increasing due to continuous enlarging of pore size by more KOH. As shown in Table 2, the pore volume, mesoporosity and average pore size all increase gradually with increasing KOH/coke ratio from 1:1 to 5:1. It is reported that relatively

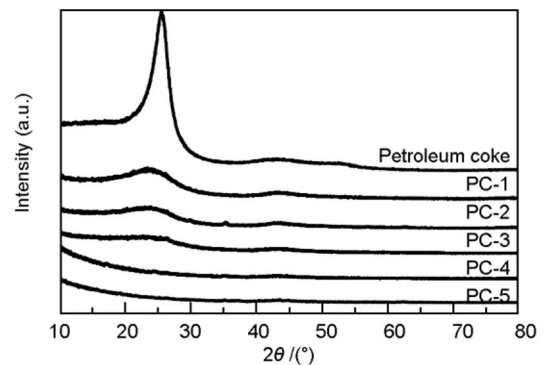


Fig. 2 XRD patterns of petroleum coke and PCs.

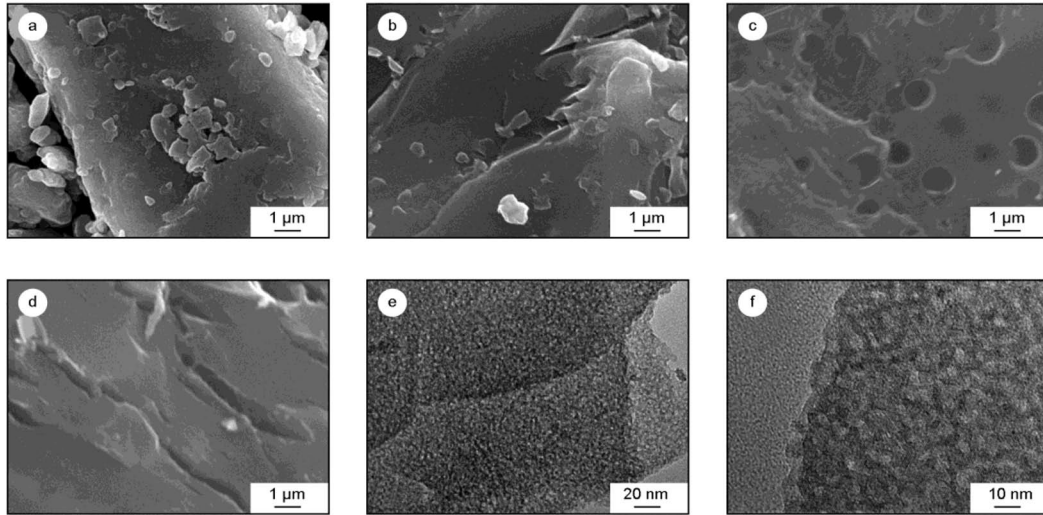


Fig. 3 SEM images of petroleum (a) coke, (b) PC-1, (c) PC-4 and (d) PC-5; (e, f) TEM images of PC-5.

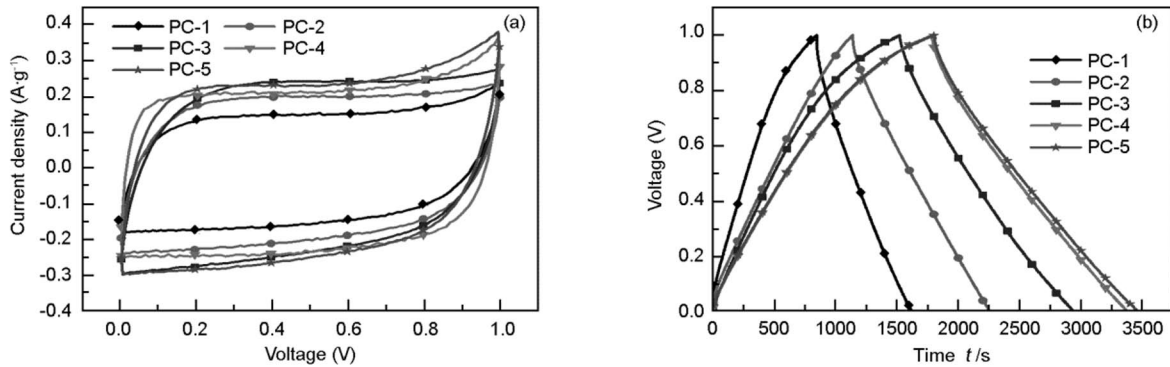


Fig. 4 (a) Cyclic voltammety curves of PC electrodes at a scan rate of 2 mV s^{-1} in a 6 M KOH aqueous electrolyte; (b) charge–discharge curves of PC electrodes at a current density of 50 mA g^{-1} in a 6 M KOH aqueous electrolyte.

big pores and high surface area of PCs are beneficial for electrochemical performance^[15]. The mesoporosity of PC-5 reaches 67.0%, much bigger than 8.8% of PC-1, while the specific surface area of PC-5 is as high as $2842 \text{ m}^2 \cdot \text{g}^{-1}$, indicating it is a good electrode material.

In order to detect the effects of KOH/coke ratios on the structure of PCs, XRD was employed to investigate the crystalline structure of the raw petroleum coke and PCs prepared at different KOH/coke ratios. Fig. 2 gives the XRD patterns of all samples. The crystalline structure of carbonaceous materials can be characterized by 2θ at 26° and 43° . The peak (002) at 26° for petroleum coke is fairly narrow and sharp, indicating large crystalline size in petroleum coke^[26]. As the KOH/coke ratio increases from 1:1 to 5:1, the (002) peak gradually becomes broad and weak, finally almost disappears at 4:1 and 5:1, indicating that the KOH destroys the crystalline structure of petroleum coke during activation. The phenomenon also can be seen from the SEM and TEM images as shown in Fig. 3. After activated at high KOH/coke ratios, the surface of PC-4 (Fig. 3c) or PC-5 (Fig. 3d) appears some big pores or slits compared to raw petroleum coke (Fig. 3a) and PC-1 (Fig. 3b). Figs 3e and 3f are the TEM images of PC-5, in which micropores and mesopores can be clearly seen.

The plentiful pores in PCs are believed to be beneficial for their electrochemical performance.

Fig. 4a displays the cyclic voltammety curves (scan rate 2 mV s^{-1}) of all the PC electrodes in a 6 M KOH aqueous electrolyte. The sweep curves are all in rectangular shape, a typical EDLC characteristic.

Fig. 4b shows the galvanostatic charge/discharge curves of PC electrodes at current density of $50 \text{ mA} \cdot \text{g}^{-1}$ in a 6 M KOH aqueous electrolyte. All curves exhibit the typical symmetrical charge–discharge pattern, indicating that PC electrodes have the typical capacitive behavior. The results of the charge–discharge test are in accordance with that from the CV measurements, as shown in Fig. 4(a). The specific capacitance of PC electrodes ($C, \text{ F} \cdot \text{g}^{-1}$) can be calculated from the slope of the discharge curve according to the following equation^[27].

$$C = I/k/m \quad (2)$$

Where, I is the discharge current, k is the slope of the discharge curve, and m is the mass of the active material in electrode. The dependence of specific capacitance on the current density for PCs is shown in Fig. 5(a). The specific

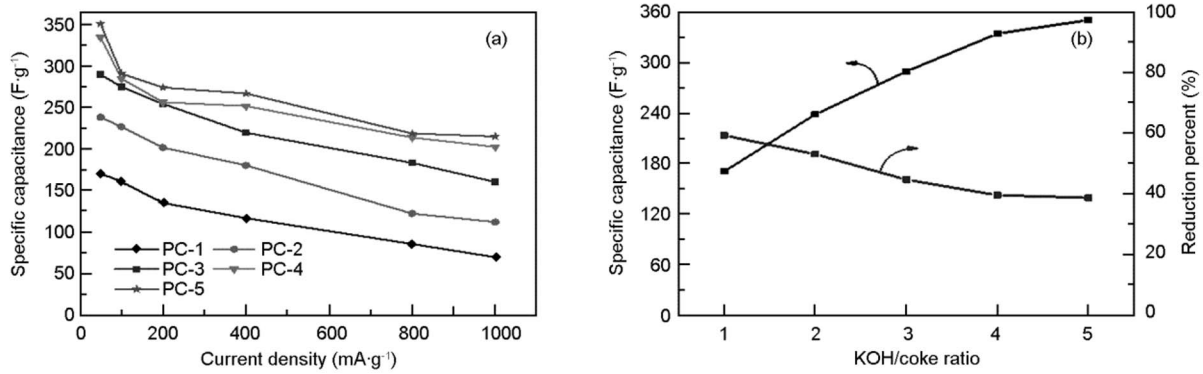


Fig. 5 (a) Specific capacitance of PC electrodes versus current density in 6 M KOH aqueous electrolyte; (b) specific capacitance and its reduction percent versus the KOH/coke ratio.

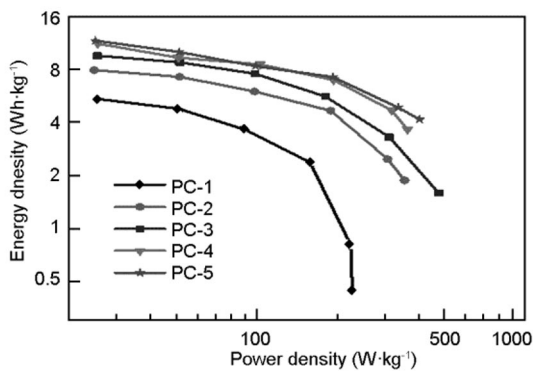


Fig. 6 Energy density versus power density of PC electrodes in a 6 M KOH aqueous electrolyte.

capacitance of PC electrodes at 50 mA·g⁻¹ increases from 170 to 350 F·g⁻¹ with increasing the KOH/coke ratio and reaches a maximum at the KOH/coke ratio of 5:1 (PC-5). Although PC-3 has the biggest surface area, the specific capacitances of PC-4 and PC-5 are bigger than that of PC-3, indicating the development of pore size and volume promotes the growth of capacitance, especially at high current densities. PC-5 electrode has the biggest specific capacitances at all current densities compared with other PC electrodes, which should be attributed to the enhanced pore size appropriate for EDL formation. The capacitance of PC-5 is 350 F·g⁻¹, much higher

than 220 F·g⁻¹ of PCs with large specific surface areas (>3000 m²·g⁻¹) in Ref^[28].

Generally, the increase in the discharge current density leads to a decrease in specific capacitance. Those decreases are ascribed to the partial inaccessibility of some electrolyte ions into the internal micropores of electrodes, so inaccessible micropores are less effective in forming EDL. The specific capacitance of PC-1 electrode decreases by more than 59% with the discharge current density from 50 to 1 000 mA·g⁻¹, while that of PC-5 electrode is only 38% (Fig. 5b), which is should be ascribed to the high mesoporosity and the synergistic effect of the mesopores and micropores. The mesopores can act as favorable channels for penetration and transportation of electrolyte ions so that the micropores and small mesopores can store more ions, facilitating high capacitance retention and excellent rate performance at high current densities.

The energy density (E , Wh·kg⁻¹) and average power density (P , W·kg⁻¹) can be calculated by using the following equations^[2, 29].

$$E = 1/2 CV^2 \quad (3)$$

$$P = E/t \quad (4)$$

Where, V is the usable voltage (V), t is the discharge time (h).

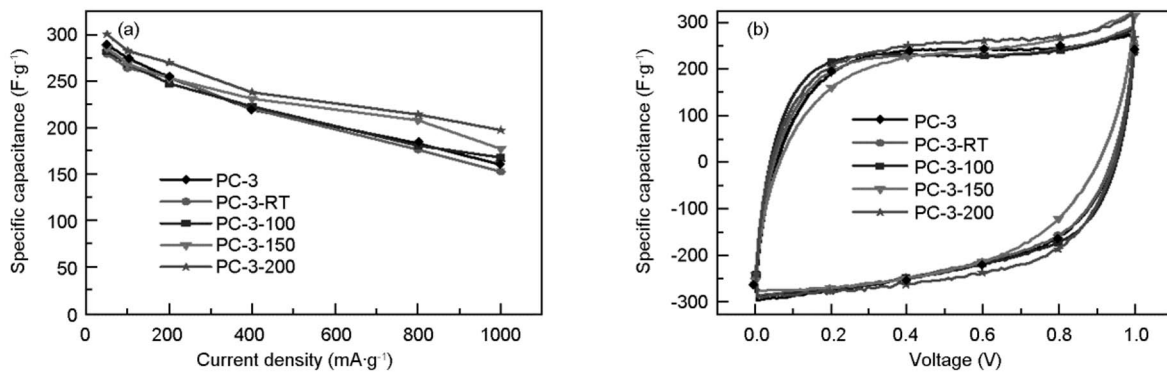


Fig. 7 (a) Specific capacitance of PC-3 and modified PC-3 electrodes versus current density in 6 M KOH aqueous electrolyte; (b) Cyclic voltammograms of PC-3 and modified PC-3 electrodes at a scan rate of 2 mV·s⁻¹ in 6 M KOH aqueous electrolyte.

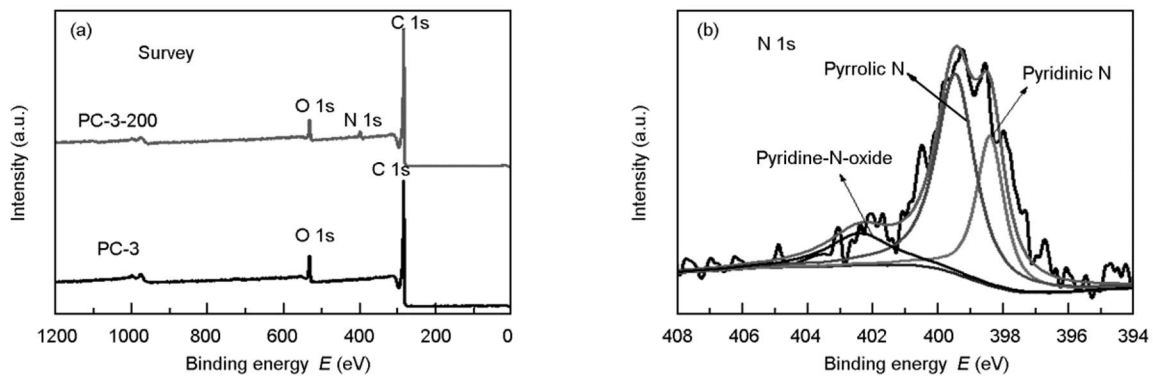


Fig. 8 (a) XPS survey spectra of PC-3 and PC-3-200 and (b) N1s XPS spectrum of PC-3-200.

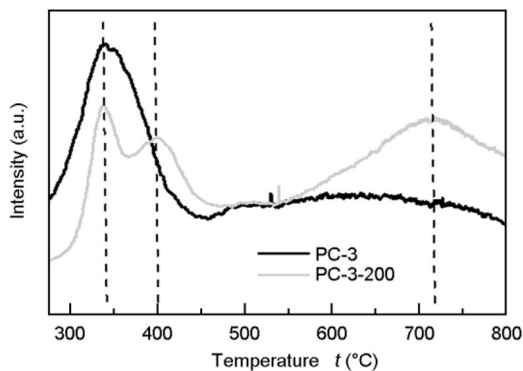


Fig. 9 CO₂-TPD curves of PC-3 and PC-3-200.

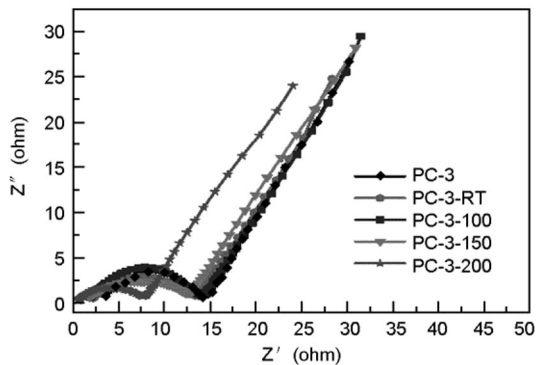


Fig. 10 Nyquist plots of the PC-3 and modified PC-3 electrodes.

The variation of the energy density of PC capacitors with the average power density is presented in Fig. 6. It can be found that the energy density of PC electrodes drops with increasing average power density for all PC electrodes, implying that less energy can be released at higher discharge rate. The energy densities of PC-2, PC-3, PC-4 and PC-5 are obviously higher than that of PC-1, which can be attributed to the increasing surface area and pore volume. As the power density increases, the energy density of PC-1 electrode drops more quickly than those of the other PC electrodes. The energy density of PC-1 electrode in 6 M KOH electrolyte drops from 5.45 to 0.44 Wh·kg⁻¹ with the increase of current density from 0.05 to 1 A·g⁻¹. For PC-5 electrode, the energy

density drops from 11.67 to 4.16 Wh·kg⁻¹, revealing the excellent rate capability of PC-5. Except for the bigger surface area and pore volume, the larger pore size and higher mesopore percentage of PCs are responsible for their bigger energy density at higher current density.

Although PC-3 has the biggest specific surface area, its surface area is not utilized adequately. In order to improve the electrochemical performance of PC-3 electrode, hydrothermal modifications by ammonia at different temperatures have been studied. Fig. 7a gives the dependence of specific capacitance on the current density for PC-3 and modified PC-3 electrodes in 6 M KOH solution. The capacitance of PC electrodes increases slightly with the increasing hydrothermal temperature, which agrees with the CV results in Fig. 7b. Especially at 200 °C, the capacitance of PC-3-200 can reach 300 F·g⁻¹ at a current density of 50 mA·g⁻¹, and can keep 200 F·g⁻¹ at 1 000 mA·g⁻¹. Keep in mind that the capacitance is 289 F·g⁻¹ at 50 mA·g⁻¹ and 150 F·g⁻¹ at 1 000 mA·g⁻¹ for PC-3 electrode, the hydrothermal modification in ammonia at 200 °C can effectively improve the capacitance of PC-3 at high discharge current density, which could be ascribed to the doped nitrogen by the hydrothermal modifications of PC-3 in ammonia.

The change of surface properties of PC-3 and modified PC-3-200 can be determined by XPS, as presented in Fig. 8. Fig. 8a compares the XPS survey spectra of PC-3 and PC-3-200. Compared to PC-3, in addition to the peaks of C1s and O1s, a N1s peak at 399.1 eV appears on PC-3-200, which demonstrates the successful N-doping with the hydrothermal modification of PC-3 in ammonia. The N1s peak can be fitted to investigate the types of nitrogen-containing groups. As shown in Fig. 8b, three different peaks at about 398.4, 399.5 and 402.4 eV could be attributed to pyridinic N, pyrrolic N and pyridine-N-oxide, respectively^[30-32]. These introduced N species can not only induce the extra pseudo-capacitance to increase the specific capacitance, but also improve the hydrophilicity of the carbon surface to facilitate the wettability of the pore with electrolyte^[22, 31]. Therefore, after hydrothermal modification by ammonia, PC-3-200 exhibits a higher specific capacitance than PC-3. Otherwise, the doped-N

can increase basic groups on PC. The previous research has proved the direct relationship between the number of basic groups and capacitance particularly at high current densities^[33]. To make sure the change of basic groups on PC caused by hydrothermal modification in ammonia, CO₂-TPD has been used to analyze PC-3 and PC-3-200. As can be seen in Fig. 9, two new peaks appear around 400 °C and 720 °C for PC-3-200, revealing that new and strong basic groups are formed by hydrothermal modification in ammonia.

In order to make sure why nitrogen-doped PC-3-200 electrode exhibits better electrochemical performance in comparison with PC-3 electrode, electrochemical impedance spectra were measured. The Nyquist plots of PC electrodes in 6 M KOH are given in Fig. 10. All plots exhibit a near vertical line in the low frequency range, showing almost purely capacitive behavior. The semicircle at high frequency regions is indicative of interfacial charge transfer resistance, and a small semicircle diameter presents a low charge transfer resistance and better electrical conductivity. It can be seen that all modified samples have smaller diameter than that of PC-3, and PC-3-200 has the smallest diameter, indicating the hydrothermal modification in ammonia can reduce interfacial charge transfer resistance and thus improve the conductivity. The intersections of these curves with the Z' axis (real impedance) represent the equivalent series resistance (ESR)^[34]. Based on the Nyquist plots, the ESR of PC-3, PC-3-RT, PC-3-100, PC-3-150 and PC-3-200 is 3.37, 2.40, 1.84, 1.78 and 0.62 ohm, respectively. For all the above mentioned reasons, all ammonia modified samples show much better electrochemical performance than that of PC-3. It is easily seen that hydrothermal treatment in ammonia at 200 °C is an effective method to dope nitrogen on PC and enhance the electrochemical performance of PC electrodes.

4 Conclusions

PCs with high surface areas and wide pore size distributions were prepared from petroleum coke via KOH activation. The specific surface area and pore size distribution of PCs can be adjusted by changing the mass ratio of KOH to petroleum coke. The largest specific surface area of PC reaches 2 964 m²·g⁻¹ at a KOH/coke ratio of 3:1. PC-5 prepared with the KOH/coke ratio of 5:1 can simultaneously keep a high specific surface area (2 842 m²·g⁻¹) and high mesoporosity (67.0%). With increasing KOH/coke ratio from 1:1 to 5:1, the specific capacitance of PC electrodes increases from 170 to 350 F·g⁻¹ at a current density of 50 mA·g⁻¹ in 6 M KOH, while the reduction percentage of the capacitance decreases from 59% to 38% with increasing current density from 50 to 1 000 mA·g⁻¹. PC-5 electrode has the biggest specific capacitance at all current densities owing to beneficial EDL formation in the pores with enlarged sizes. Hydrothermal modification in ammonia at 200 °C can introduce nitrogen to PC and reduce the interfacial charge transfer resistance and equivalent series resistance of PC electrodes, resulting in an improvement on their electrochemical performance, especially

at a high discharge current density. KOH activation with subsequent ammonia hydrothermal modification is proved to be a simple yet efficient approach to prepare cost-effective PCs for supercapacitors.

References

- [1] Burke A. Ultracapacitors: Why, how, and where is the technology [J]. *Journal of Power Sources*, 2000, 91(1): 37-50.
- [2] Lewandowski A, Galinski M. Practical and theoretical limits for electrochemical double-layer capacitors [J]. *Journal of Power Sources*, 2007, 173(2): 822-828.
- [3] Choi N S, Chen Z, Freunberger S A, et al. Challenges facing lithium batteries and electrical double-layer capacitors [J]. *Angewandte Chemie International Edition*, 2012, 51(40): 9994-10024.
- [4] Simon P, Gogotsi Y. Materials for electrochemical capacitors [J]. *Nature Materials*, 2008, 7(11): 845-854.
- [5] Wang G, Zhang L, Zhang J. A review of electrode materials for electrochemical supercapacitors [J]. *Chemical Society Reviews*, 2012, 41(2): 797-828.
- [6] Zhai Y, Dou Y, Zhao D, et al. Carbon materials for chemical capacitive energy storage [J]. *Advanced Materials*, 2011, 23(42): 4828-4850.
- [7] Inagaki M, Konno H, Tanaike O. Carbon materials for electrochemical capacitors [J]. *Journal of Power Sources*, 2010, 195(24): 7880-7903.
- [8] Frackowiak E, Béguin F. Carbon materials for the electrochemical storage of energy in capacitors [J]. *Carbon*, 2001, 39(6): 937-950.
- [9] Pandolfo A G, Hollenkamp A F. Carbon properties and their role in supercapacitors [J]. *Journal of Power Sources*, 2006, 157(1): 11-27.
- [10] Qu D. Studies of the activated carbons used in double-layer supercapacitors [J]. *Journal of Power Sources*, 2002, 109(2): 403-411.
- [11] Chmiola J, Yushin G, Gogotsi Y, et al. Anomalous increase in carbon capacitance at pore sizes less than 1 nanometer [J]. *Science*, 2006, 313(5794): 1760-1763.
- [12] Zhou H, Zhu S, Hibino M, et al. Electrochemical capacitance of self-ordered mesoporous carbon [J]. *Journal of Power Sources*, 2003, 122(2): 219-223.
- [13] Li L, Song H, Chen X. Pore characteristics and electrochemical performance of ordered mesoporous carbons for electric double-layer capacitors [J]. *Electrochimica Acta*, 2006, 51(26): 5715-5720.
- [14] Wang J, Xue C, Lv Y, et al. Kilogram-scale synthesis of ordered mesoporous carbons and their electrochemical performance [J].

- Carbon, 2011, 49(13): 4580-4588.
- [15] Wu M, Ai P, Tan M, et al. Synthesis of starch-derived mesoporous carbon for electric double layer capacitor [J]. *Chemical Engineering Journal*, 2014, 245: 166-172.
- [16] Ryoo R, Joo S H, Kruk M, et al. Ordered Mesoporous Carbons [J]. *Advanced Materials*, 2001, 13(9): 677-681.
- [17] Fuertes A B, Nevskaya D M. Control of mesoporous structure of carbons synthesised using a mesostructured silica as template [J]. *Microporous Mesoporous Materials*, 2003, 62(3): 177-190.
- [18] Chmiola J, Yushin G, Dash R, et al. Effect of pore size and surface area of carbide derived carbons on specific capacitance [J]. *Journal of Power Sources*, 2006, 158(1): 765-772.
- [19] Gao F, Shao G, Qu J, et al. Tailoring of porous and nitrogen-rich carbons derived from hydrochar for high-performance supercapacitor electrodes [J]. *Electrochimica Acta*, 2015, 155: 201-208.
- [20] Li B, Dai F, Xiao Q, et al. Nitrogen-doped activated carbon for a high energy hybrid supercapacitor [J]. *Energy & Environmental Science*, 2016, 9(1): 102-106.
- [21] Chen L, Zhang X, Liang H, et al. Synthesis of nitrogen-doped porous carbon nanofibers as an efficient electrode material for supercapacitors [J]. *ACS Nano*, 2012, 6(8): 7092-7102.
- [22] Zhao L, Fan L, Zhou M, et al. Nitrogen-containing hydrothermal carbons with superior performance in supercapacitors [J]. *Advanced Materials*, 2010, 22(45): 5202-5206.
- [23] Wu M, Zha Q, Qiu J, et al. Preparation of porous carbons from petroleum coke by different activation methods [J]. *Fuel*, 2005, 84(14-15): 1992-1997.
- [24] Lu C, Xu S, Gan Y, et al. Effect of pre-carbonization of petroleum cokes on chemical activation process with KOH [J]. *Carbon*, 2005, 43(11): 2295-2301.
- [25] He X, Geng Y, Qiu J, et al. Effect of activation time on the properties of activated carbons prepared by microwave-assisted activation for electric double layer capacitors [J]. *Carbon*, 2010, 48(5): 1662-1669.
- [26] Xu B, Chen Y, Wei G, et al. Activated carbon with high capacitance prepared by NaOH activation for supercapacitors [J]. *Materials Chemistry and Physics*, 2010, 124(1): 504-509.
- [27] Zhao Q, Wang X, Wu C, et al. Supercapacitive performance of hierarchical porous carbon microspheres prepared by simple one-pot method [J]. *Journal of Power Sources*, 2014, 254(0): 10-17.
- [28] Lozano-Castelló D, Cazorla-Amorós D, Linares-Solano A, et al. Influence of pore structure and surface chemistry on electric double layer capacitance in non-aqueous electrolyte [J]. *Carbon*, 2003, 41(9): 1765-1775.
- [29] Lei Z, Liu Z, Wang H, et al. A high-energy-density supercapacitor with graphene-CMK-5 as the electrode and ionic liquid as the electrolyte [J]. *Journal of Materials Chemistry A*, 2013, 1(6): 2313-2321.
- [30] Wu M, Wang Y, Wu W, et al. Preparation of functionalized water-soluble photoluminescent carbon quantum dots from petroleum coke [J]. *Carbon*, 2014, 78: 480-489.
- [31] Fan L, Chen T, Song W, et al. High nitrogen-containing cotton derived 3D porous carbon frameworks for high-performance supercapacitors [J]. *Scientific Reports*, 2015, 5: 15388.
- [32] Zhou J, Zhang Z, Xing W, et al. Nitrogen-doped hierarchical porous carbon materials prepared from meta-aminophenol formaldehyde resin for supercapacitor with high rate performance [J]. *Electrochimica Acta*, 2015, 153: 68-75.
- [33] Sereych M, Hulicova-Jurcakova D, Lu G, et al. Surface functional groups of carbons and the effects of their chemical character, density and accessibility to ions on electrochemical performance [J]. *Carbon*, 2008, 46(11): 1475-1488.
- [34] Pendashteh A, Mousavi M F, Rahmanifar M S. Fabrication of anchored copper oxide nanoparticles on graphene oxide nanosheets via an electrostatic coprecipitation and its application as supercapacitor [J]. *Electrochimica Acta*, 2013, 88: 347-357.